Ther Adv Cardiovasc Dis
2019, Vol. 13: 1–13
DOI: 10.1177/1753944719841795

Dysregulation of proangiogeneic factors in pressure-overload left-ventricular hypertrophy results in inadequate capillary growth

Mohamed Zeriouh*, Anton Sabashnikov*, Arne Tenbrock*, Klaus Neef, Julia Merkle, Kaveh Eghbalzadeh, Carolyn Weber, Oliver J. Liakopoulos, Antje-Christin Deppe, Christof Stamm, Douglas B. Cowan, Thorsten Wahlers and Yeong-Hoon Choi

Abstract

Background: Pressure-overload left-ventricular hypertrophy (LVH) is an increasingly prevalent pathological condition of the myocardial muscle and an independent risk factor for a variety of cardiac diseases. We investigated changes in expression levels of proangiogeneic genes in a small animal model of LVH.

Methods: Myocardial hypertrophy was induced by transaortic constriction (TAC) in C57BL/6 mice and compared with sham-operated controls. The myocardial expression levels of vascular endothelial growth factor (VEGF), its receptors (KDR and FLT-1), stromal-cell-derived factor 1 (SDF1) and the transcription factors hypoxia-inducible factor-1 and 2 (HIF1 and HIF2) were analyzed by quantitative polymerase chain reaction over the course of 25 weeks. Histological sections were stained for caveolin-1 to visualize endothelial cells and determine the capillary density. The left-ventricular morphology and function were assessed weekly by electrocardiogram-gated magnetic resonance imaging.

Results: The heart weight of TAC animals increased significantly from week 4 to 25 ($p = 0.005$) compared with sham-treated animals. At 1 day after TAC, the expression of VEGF and SDF1 also increased, but was downregulated again after 1 week. The expression of HIF2 was significantly downregulated after 1 week and remained at a lower level in the subsequent weeks. The expression level of FLT-1 was also significantly decreased 1 week after TAC. HIF-1 and KDR showed similar changes compared with sham-operated animals. However, the expression levels of HIF1 after 4 and 8 weeks were significantly decreased compared with day 1. KDR changes were significantly decreased after 1, 2, 4, 8 and 25 weeks compared with week 3. After 4 weeks post-TAC, the size of the capillary vessels increased ($p = 0.005$) while the capillary density itself decreased (TAC: 2143 ± 293 /mm^2 *versus* sham: 2531 ± 321 /mm^2; $p = 0.021$). Starting from week 4, the left-ventricular ejection fraction decreased compared with controls ($p = 0.049$).

Conclusions: The decrease in capillary density in the hypertrophic myocardium appears to be linked to the dysregulation in the expression of proangiogeneic factors. The results suggest that overcoming this dysregulation may lead to reconstitution of capillary density in the hypertrophic heart, and thus be beneficial for cardiac function and survival.

Keywords: ejection fraction, gene expression, left-ventricular hypertrophy, proangiogenic factors

Received: 16 October 2017; revised manuscript accepted: 13 March 2019.

Correspondence to:
Yeong-Hoon Choi
Department of Cardiothoracic Surgery – Heart Center of the University, University of Cologne, Kerpener Straße 62, 50924 Cologne, Germany

Center of Molecular Medicine Cologne, University of Cologne, Cologne, Germany
yh.choi@uk-koeln.de

Mohamed Zeriouh
Anton Sabashnikov
Arne Tenbrock
Klaus Neef
Julia Merkle
Kaveh Eghbalzadeh
Carolyn Weber
Oliver J. Liakopoulos
Antje-Christin Deppe
Department of Cardiothoracic Surgery, University of Cologne, Cologne, Germany

Christof Stamm
Berlin–Brandenburg Center for Regenerative Therapies, Berlin, Germany

Douglas B. Cowan
Department of Anesthesiology, Perioperative and Pain Medicine, Children's Hospital Boston and Harvard Medical School, Boston, MA, USA

Thorsten Wahlers
Department of Cardiothoracic Surgery, University of Cologne, Cologne, Germany

Center of Molecular Medicine Cologne, University of Cologne, Cologne, Germany

Yeong-Hoon Choi
Center of Molecular Medicine Cologne, University of Cologne, Cologne, Germany

*The authors contributed equally and share the first authorship.

Introduction

Pressure-overload left-ventricular (LV) hypertrophy as observed in patients with, that is, aortic stenosis or arterial hypertension, is the most common secondary diagnosis in cardiovascular patients.[1] If untreated, the hypertrophy progresses from concentric to eccentric hypertrophy resulting in contractile dysfunction and heart failure.[2] Furthermore, hypertrophic myocardium shows an increased susceptibility to an ischemia/reperfusion injury.[3,4] This results from an altered intracellular calcium handling and impaired reconstitution of adenosine triphosphate (ATP) levels upon reperfusion, decreased glucose uptake of cardiomyocytes[5,6] and a decreased myocardial capillary density. Thus, an increased diffusion distance and limited energy substrates supply result.[7,8]

Hypoxia-inducible transcription factors (HIF) are dimeric, basic helix-loop-helix transcription factors consisting of an oxygen-dependent α-subunit and a stable β-subunit.[9,10] HIF is the key regulator of a diversity of genes affecting the cellular response to hypoxia, including oxygen delivery, metabolism, cell survival and angiogenesis.[9] Under hypoxic conditions, the transcription of several genes, including glycolysis enzymes (allowing ATP synthesis of oxygen independently), vascular endothelial growth factor (VEGF) and stromal-cell-derived factor-1α (SDF-1α) promoting angiogenesis is upregulated.[11–13]

HIF-1 plays an integral role in the body's response to low oxygen concentrations, or hypoxia.[14] HIF-1 is among the primary genes involved in the homeostatic process, which can increase vascularization in hypoxic areas such as localized ischemia and tumors.[15] It is a transcription factor for dozens of target genes; HIF-1 is also a crucial physiological regulator of homeostasis, vascularization, and anaerobic metabolism.[16] Furthermore, HIF-1 is increasingly studied because of its perceived therapeutic potential. As it causes angiogenesis, enhancement of this gene within ischemic patients could promote the vessel proliferation needed for oxygenation.[15,17] Gene therapy to achieve both vessel proliferation and tumor regression has been demonstrated in animal studies but requires significant improvement and modification before becoming commercially available.[14,15]

In myocardial hypertrophy, the decreased capillary density may lead to tissue hypoxia, inducing HIF-dependent signaling. Indeed, in diabetic conditions, a recent study shows that HIF-1 might play an important role in diabetic cardiomyopathy. Hypoxia and oxidative stress are frequently caused by hyperglycemia and therefore lead to diabetes-induced reduction in cardiac capillaries.[7]

In the present study, we investigated the myocardial expression of proangiogenic factors in a murine animal model of pressure-overload LV hypertrophy. The main goal was to determine specifically alterations of gene-expression levels of the vascular growth factor and the corresponding receptors. These may be potential targets for future therapeutic approaches to improve the myocardial capillarization in the failing hypertrophic heart.

Material and methods

Animal model

Animals received humane care in compliance with the EU directive 2010/63/EU for animal experiments and the Principles of Laboratory Animal Care formulated by the National Society of Medical Research and The Guide for the Care and Use of Laboratory Animals prepared by The National Academy of Sciences and published by The National Institutes of Health (NIH Publication no. 86-23, revised 1996). All experiments have been approved by the Office for Animal Care and Use of the State Government (Landesamt für Natur, Umwelt und Verbraucherschutz Nordrhein-Westfalen, LANUV). We analyzed 21 mice with transaortic constriction (TAC) and 21 mice with sham procedure. The groups were observed at 7 points of time (day 1, week 1, 2, 3, 4, 8 and 25). Death rate was 12% (totaling 37 animals).

Surgical procedures

TAC was performed through a minimally invasive transjugular approach as described previously.[18] In brief, 8-week-old adult C57BL/6 mice (18–22 g, Charles River, Sulzfeld, Germany) were anesthetized with intraperitoneal administration of ketamine (150 mg/kg, Pfizer, Berlin, Germany) and xylazine (10 mg/kg, Bayer, Leverkusen, Germany). The aortic arch was visualized through a minimally invasive transjugular incision under spontaneous breathing. A 6-0 silk suture (Ethicon, Norderstedt, Germany) was placed around the aortic arch and a 27-gauge cannula was then placed next to the aortic arch as a place holder.

The suture was tightly tied around the needle and the aorta. After ligation, the cannula was quickly removed. The skin was closed, and mice were allowed to recover on a warming pad until they were fully awake. The control animals underwent a sham procedure, including the thoracotomy and manipulation of the aorta. After surgery, mice were treated with subcutaneous buprenorphine for pain (0.1 mg/kg). First infusion of buprenorphine was 30 min before surgery. Afterwards, buprenorphine was infused every 12 h for a maximum of 5 days. Every day, mice were checked, and pain medication was administered, if necessary.

Tissue harvest, total RNA extraction, and reverse transcription

Mice were euthanized and hearts were excised on day 1 and on week 1, 2, 3, 4, 8 and 25 after TAC in order to quantify changes in expression of genes involved in angiogenesis. The hearts were perfused with cold phosphate-buffered solution (4°C) (Sigma Aldrich, St. Louis, MO, USA). After embedding in Tissue-Tek (Sakura, Staufen, Germany) the samples were snap frozen in 2-methylbutane and stored at −80°C. The total ribonucleic acid (RNA) was isolated from isolated LV samples (20 midventricular cryosections, 10 μm) using the TRIzol reagent (Invitrogen, Carlsbad, CA, USA) according to the manufacturer's instructions, followed by deoxyribonucleic acidase (Invitrogen) treatment. RNA concentrations and quality were determined by fluorometry (Qubit, Invitrogen). Reverse transcription was performed with 1 μg RNA per each reaction [High-Capacity cDNA Reverse-Transcription Kit, Applied Bioscience (ABI), Darmstadt, Germany] and complementary deoxyribonucleic acid (cDNA) was stored at −20°C.

Quantitative polymerase chain reaction

Gene-expression levels of VEGF and SDF-1, the receptors FLT-1 and KDR as well as the transcription factors HIF-1α and 2α were determined by quantitative polymerase chain reaction (PCR) using the Power SYBR Green PCR Mastermix and the 7300 real-time PCR system (both ABI). The sequences of the oligonucleotide primers (Invitrogen) are shown in Table 1. Each real-time PCR assay was run in triplicates (10 ng cDNA template and 300 nmol/l primers in a final reaction volume of 20 μl). Cycling parameters were: 50°C for 2 min, 95°C for 10 min to activate DNA polymerase, and then 40 cycles of 95°C for 15 s and 60°C for 1 min. Melting curve analysis was performed to rule out the occurrence of PCR side products. Real-time PCR efficiency (E) of each primer set was assessed from standard curves of serial cDNA dilutions according to the equation $E = 1^{(-1/\text{slope})}$.

Reactions were only included when PCR efficiency was confirmed at 90–110%. Cycle threshold (Ct) values were determined using the SDS software (ABI) and ΔCt (endogenous control: β-actin) and ΔΔCt (reference group: healthy animals) were calculated. Relative expression (RE) was calculated according to the equation $RE = 2^{(-\Delta\Delta Ct)}$.

Capillary density

To quantify myocardial capillary density, the animals were sacrificed 4 weeks after surgery. After cryosectioning (10 μm) the histological samples were stained using a monoclonal antibody against caveolin-1 (1:100, Acris Antibodies, Herford, Germany) and visualized by an Alexa Fluor 488 (Thermo Fisher Scientific, Waltham, MA, USA) conjugated secondary goat antimouse antibody (1:200, Invitrogen). For nuclear counterstaining, the slides were incubated with 4',6-diamidino-2-phenylindole (DAPI, 1:1000, Invitrogen). The slides were visualized using a Nikon Eclipse Ti-U microscope (Nikon, Düsseldorf, Germany) equipped with visible/ultraviolet/fluorescent objectives (4–100×), xenon light source and appropriate excitation/emission filter sets. Images were acquired with a Nikon cooled CCD camera and analyzed using the Nikon software NIS elements BR 3.0 (Nikon). In order to determine the myocardial capillary density, 15 randomly selected fields of cross-sectioned capillaries in the LV free wall were examined.

MR image acquisition

The cardiac function was assessed *in vivo* using a clinical 3.0 T magnetic resonance imaging (MRI) scanner (80 mT/m maximum strength, slew rate: 200 mT × ms/m, Intera Achieva, Phillips Medical Systems, Best, Netherlands) as described previously.[19] To enhance signal-to-noise ratio, the MRI scanner was equipped with a dedicated experimental small animal solenoid coil (Phillips). Serial cardiac MRI scans were performed weekly for 25 weeks after TAC. Mice

Table 1. Oligonucleotide primers for real-time PCR.

Gene	Primer sequence (5'–3')		NCBI Reference sequence
ß-Actin	F	CCACACCCGCCACCAGTTCG	NM_007393.3
	R	TACAGCCCGGGGAGCATCGT	
FLT-1/VEGFR1	F	GCTGTTTCGGGCCCCCTTCC	NM_010228.3
	R	GCCTCAGAAGCCAAGCGCCA	
KDR/VEGFR2	F	GCGCGAGGTGCAGGATGGAG	NM_010612.2
	R	TCCCGCTGTCCCCTGCAAGT	
SDF-1	F	GCCCTTCAGATTGTTGCACGGC	NM_001012477.1
	R	CACTGCGGTCCATCGGCAGG	
VEGFa	F	CCAGGCTGCACCCACGACAG	NM_001025250.3
	R	CGGACGGCAGTAGCTTCGCT	
HIF-1α	F	GAAGACAACGCGGGCACCGA	NM_010431.2
	R	TGCTTCGCCGAGATCTTGCTGC	
HIF-2α	F	GCCAAGACTGGGTTCCCGCC	NM_010137.3
	R	GGCTCGAACGATGGCCCCAG	

NCBI, National Center of Biotechnology Information; HIF, hypoxia-inducible transcription factor; SDF, stromal-cell-derived factor; VEGF, vascular endothelial growth factor.

were anesthetized with 1.25% isoflurane (1 l/min O_2, Abbott, Abbott Park, IL, USA). Long-axis images of the left ventricle were obtained by electrocardiogram (ECG)-gated sagittal scans. Cardiac function was assessed by ECG-gated acquisition of transversal images of 6 slices with 12 cardiac phases of the left ventricle between the end-systolic and end-diastolic state. Normothermic levels were achieved by using a heating system integrated in the solenoid coil. The MRI assessment was performed weekly. The transversal MRI images covering the complete left ventricle were used for semiautomated assessment of endocardial and epicardial contours. The LV ejection fraction (LVEF) and LV mass determined as described previously.[19,20] Data were analyzed independently by three experienced investigators.

Statistical analysis

Numeric data are expressed as mean ± one standard deviation. The statistical analyses were performed using the SPSS software package (release 20, IBM, Somers, NY, USA). The data derived from MRI and PCR were tested by two-way repeated-measure analysis of variance followed by a Holm–Sidak *post hoc* test for multiple comparisons. The capillary density data were tested using the unpaired student *t* test. A two-tailed probability value $\leqslant 0.05$ was considered to indicate statistical significance.

Results

Magnetic resonance imaging

The hearts from mice 1 week post-TAC showed clear evidence of cardiac hypertrophy compared with those of the control group, as indicated by increased heart weight and decreased LVEF [Figure 1(b)].

In the MRI, the LVEF was measured weekly. Over time, there was no change of the LVEF in TAC animals (week 1 *versus* week 2: $p = 0.995$,

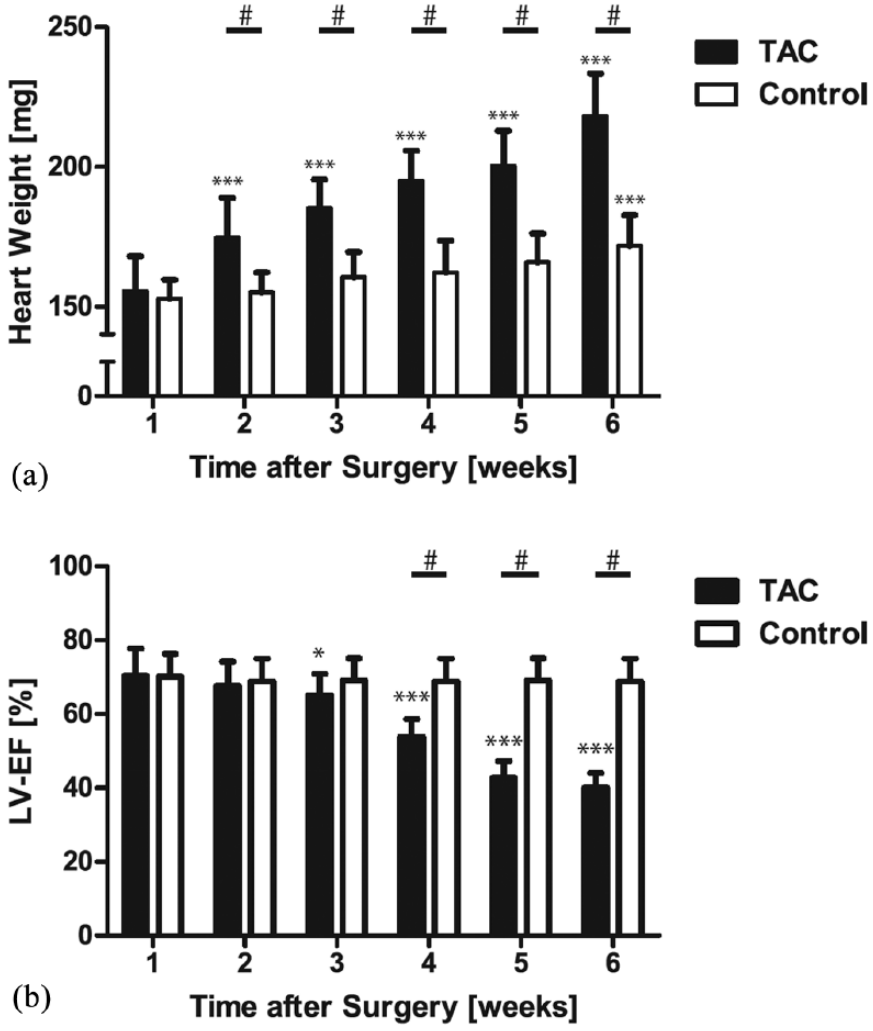

Figure 1. Cumulative data of progression of left-ventricular heart failure and hypertrophy after transverse aortic constriction.
Heart failure (a) and hypertrophy [heart weight, (b)] after transverse aortic constriction. While the LV heart weight increases significantly already after week 2, the LV function is preserved until week 3 (compensated hypertrophy) and deteriorates afterwards. The increase of heart weight in the control group is caused by the physiologic growth of the animals.
$^{*}p < 0.05$ *versus* 1 week.
$^{***}p < 0.005$ *versus* 1 week.
$^{\#}p < 0.001$.
LV, left ventricular; LVEF, left-ventricular ejection fraction; TAC, transverse aortic constriction.

week 1 *versus* week 3: $p = 0.927$). However, when comparing 1 week to 4 weeks post-TAC, ($p = 0.049$), to 5 weeks ($p = 0.021$) and to subsequent weeks ($p < 0.005$), the LVEF was statistically significant decreased.

While ventricular hypertrophy was detectable 2 weeks after TAC as indicated by increased heart weight, the LV function did not reveal any difference up to 4 weeks post-TAC (compensated hypertrophy). The compensated stage was followed by development of severe heart failure, characterized by increased heart weight and decreased left ventricular function [Figure 1(a)].

Myocardial capillaries

Immunohistochemical analyses revealed a prominent decrease in capillary density in TAC animals compared with control animals at 4 weeks after TAC ($2693.1 \pm 275.4/mm^2$ *versus* $3159.1 \pm 296.2/mm^2$; $p = 0.002$). A representative

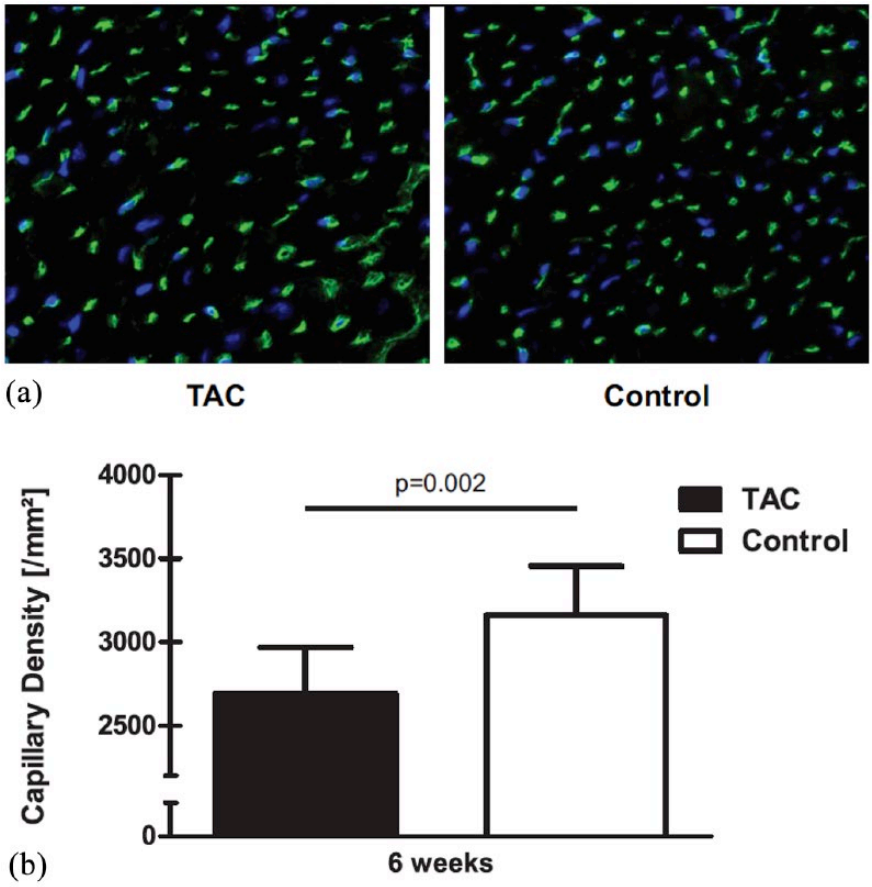

Figure 2. Selected representative field of the left-ventricular free wall of tissue cross-sections 25 weeks after transverse aortic constriction.
(a) The image shows the visualized capillary vessels using fluorescence detection. The banded (TAC) animals showed a decreased capillary density; (b) bar graph shows quantitative analysis of capillary per mm². Capillary density was significantly decreased in myocardial tissue from TAC animals.
TAC, transverse aortic constriction.

photomicrograph and the quantitative analysis are shown in Figure 2.

Also, capillary circumference was significantly increased ($p = 0.005$) between TAC (mean = 20μm) and sham animals (mean = 19 μm).

Gene-expression analysis

Compared with control animals, VEGF expression [Figure 3(a)] showed an important increase for TAC-operated animals after 1 day (2.1-fold; $p < 0.001$) and 3 weeks (1.5-fold; $p = 0.014$). Notably, these two peaks of expression levels were significantly higher compared with all other time points. However, there was a strong decrease in expression from week 3 to 4 after TAC (0.1-fold, $p = 0.005$) and expression levels remained lower from week 8 to 25 compared with earlier time points (all $p = 0.005$).

Similarly, the expression of SDF-1 [Figure 3(b)] was increased significantly only at day 1 after TAC compared with control animals (3.1-fold; $p < 0.001$). Furthermore, this expression maximum at day 1 was higher compared with all other time points of analysis from week 1 to 25 (all $p < 0.001$). Similar to expression levels of VEGF, a trend for increase of expression *versus* control was observed at week 3 (1.3-fold), although not reaching statistical significance.

The expression of receptor FLT-1 [VEGF-R1; Figure 3(c)] changed only between day 1 and day

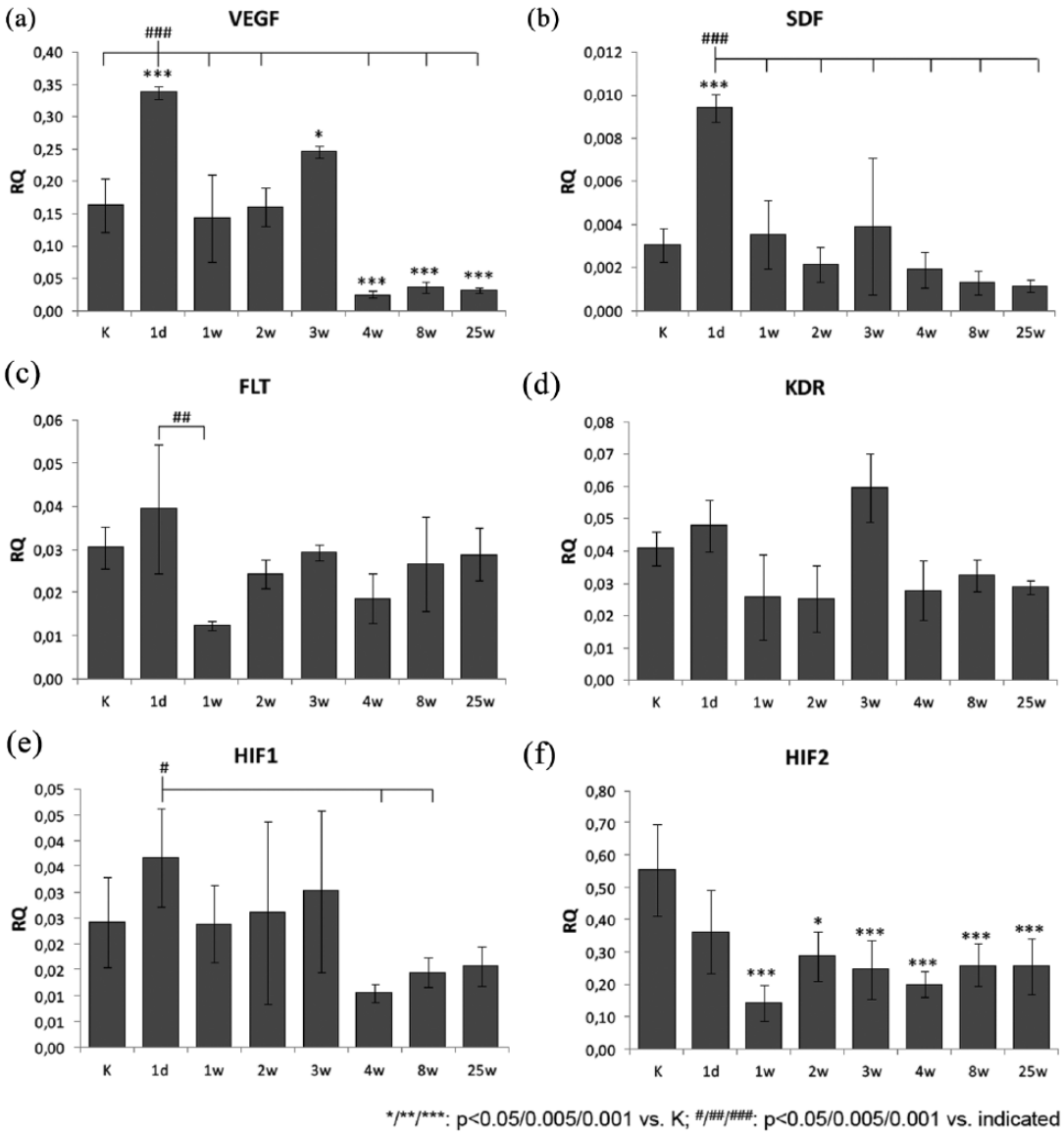

Figure 3. Expression analysis of genes with relevance for angiogenesis in the myocardium.
The plots show the myocardial gene-expression levels of proangiogenic growth factors [(a), (b); VEGF and SDF-1], transcription factors [(c), (d); HIF-1α and HIF-2 α] and VEGF-receptors [(e), (f); FLT-1/FLT-1 and KDR/KDR] of animals who underwent transverse aortic constriction (TAC) compared with sham-operated animals (K) determined by quantitative polymerase chain reaction 1 day, 1 week, 2 weeks, 3 weeks, 4 weeks, 8 weeks and 25 weeks postoperatively. The graphs (a), (c) and (e) demonstrate the relative expression (RQ) of the target gene compared with the endogenous control (β-actin) and the statistical evaluation of the differences between each group (at each time $n = 5$; analysis of variance with Bonferroni *post hoc* test for multiple comparisons). The graphs (b), (d) and (f) show the relative gene expression compared with the sham-operated control group. Demonstrating the expression of the target gene in TAC animals in comparison with the sham animals over a 3-week observation period, the expression level of the TAC group normalized to the expression level of the sham group (RQ = 1).
$^{*}p < 0.05$.
$^{**}p < 0.\ 005$.
$^{***}p < 0.001$.
$^{\#}p < 0.05$.
$^{\#\#}p < 0.005$.
$^{\#\#\#}p < 0.001$.

7 after TAC (0.5-fold; $p = 0.009$), corresponding to a 1.1-fold increase at day 1 and a 0.6-fold decrease at day 7 after TAC, compared with control animals.

Similarly, expression of receptor KDR [VEGF-R2; Figure 3(d)] showed no significant change after TAC compared with control animals, but reached an expression level maximum 3 weeks after operation, which was higher compared with animals 1, 2, 4, 8 and 25 weeks after operation (~twofold; all $p = 0.005$).

The transcription factors HIF-1 and HIF-2 showed markedly different changes of expression levels after TAC. Compared with control animals, the expression levels of HIF-1 [Figure 3(e)] showed no significant change, but showed a relative expression level maximum at day 1 after TAC, which was increased, compared with week 4 (3.5-fold; $p = 0.021$) and 8 (2.5-fold; $p = 0.035$). In the case of HIF-2 [Figure 3(f)], a significant decrease in expression level (0.26-fold; $p < 0.001$) was observed week 1 after TAC, compared with control animals. In the following course of observation from week 2 to week 24, the expression level increased moderately but remained significantly lower compared with control animals.

Generally, the observations show a strong increase of expression for growth factors VEGF and SDF already 1 day post-TAC, with a return to normal expression levels (as in control animals) at week 1. In both cases, the expression level then decreases from week 4 to levels below control animals. Regarding absolute expression levels (number of transcripts), VEGF is about 10-fold higher than SDF. The course of expression levels for receptors FLT-1 and KDR shows only moderate changes, with a notable expression minimum for FLT-1 at week 1 after TAC and a relative maximum at week 3 post-TAC for KDR. Absolute expression levels were similar for both genes throughout the observation period. In the case of the transcription factors, notable decrease in expression was observed from week 4 post-TAC for HIF-1, while HIF-2 was already decreased at day 1 after TAC and reached a relative minimum at week 1 post-TAC. Here, absolute expression levels were generally around 10-fold higher for HIF-2 compared with HIF-1.

Discussion

In this study, we validated the progression of the LV hypertrophy *in vivo* by MRI in mice. We also demonstrated that the consecutive LV dilation after 4 weeks is associated with a significant decreased LV function and cardiac decompensation, as Kaza et al. have shown in their work.[21] Previously, our group also showed that the physiological myocardial proangiogeneic response to hypoxia was prevented by pressure-overload hypertrophy.[7] Therefore, angiogenesis is important for maintaining oxygen supply in the myocardium.

Considering this, we investigated the underlying mechanisms which are responsible for failure of the myocardium to adapt. Despite the early onset of LV hypertrophy as determined at 2 weeks after TAC, resulting in a significant increase of heart weight, the LVEF remained unchanged until week 3 [see Figure 1(a) and 1(b)].

Although there is initial compensation, at 4 weeks post-TAC, hypertrophy promotes the progression of heart failure by entering through a relative decrease in capillary density in relation to myocardial ischemia. The reversal of the hypertrophy is caused mainly by a relative decrease in capillary density in relation to the resulting contractile mass. The decreased capillary density may result in a mismatch in energy supply and energy. The result is a decrease of the capillary-to-myocyte ratio and may lead to an increase in oxygen diffusion distance. In this context, VEGF plays a very important role in regulating signals for endothelial growth and capillary tubule formation by binding to its two tyrosine-kinase receptors: VEGFR1 (FLT-1) and VEGFR2 (KDR).[22] Stress and hypoxia are the main stimulators for VEGF production and release.[7,23]

In interpreting these findings, we need to focus here on gene-expression levels, where VEGFR2 (KDR) was increased significantly ($p < 0.001$) from week 2 to 3 post-TAC, while VEGFR1 (FLT-1) expression remains below that of sham animals. Although VEGF and its more physiologically relevant receptor KDR[24] were upregulated again 3 weeks after TAC, no compensative new vessel formation was yet observed. The findings suggest that a brief upregulation of VEGF results in instability of newly formed vessels, as has been reported before.[25] As it is clear that KDR is the

Table 2. LVEF and VEGFR1/2 ratio.

Post-TAC	1 day	1 week	2 weeks	3 weeks	4 weeks	8 weeks	25 weeks
LVEF	69	70.25	67.63	65	53.88	42.75	40
FLT-1/KDR	0.82	0.482	0.976	0.492	0.679	0.821	1.003

KDR, VEGFR2; FLT-1, VEGFR1; LVEF, left-ventricular ejection fraction; TAC, transverse aortic constriction; VEGFR, vascular endothelial growth factor receptor.

primary receptor transducing the leading signals for angiogenesis by binding to VEGF,[26] it is very interesting to note that there is a significant ($p < 0.01$) falling off from week 3 to 4 [see Figure 3(d)]. Interestingly, during the expression analysis covering from 3 to 4 weeks after TAC, beyond that, as can be seen from Figure 3(a), there is also a significant decline ($p < 0.001$) of VEGF from week 3 to week 4 post-TAC. These results show a notable parallel between VEGF and KDR in up- and downregulation at the molecular level, on the gene-expression level, particularly from week 3 to 4. The role of KDR has received considerable attention as being involved in angiogenesis;[26] Reynolds and colleagues suggested that KDR interferes with the majority of all cellular responses to VEGF such as angiogenesis in cancer and embryonic vasculogenesis.[27] According to Choi and colleagues, the reduced KDR and VEGF gene expression after week 4 in this study also appear to be related to the decreased capillary density and thus result in lack of upregulation of VEGF and KDR.[7] The abrupt decrease of the ejection fraction after 4 weeks post-TAC in rabbit model is also reported by Kaza and colleagues with respect to heart failure in neonatal white rabbits that underwent aortic banding.[21] Remarkably, it is worth mentioning that in both animal models (mouse and rabbit) after exactly 4 weeks, this led to a cardiac failure.[21] These findings demonstrate that LV function was stable up to exactly 4 weeks after TAC (compensated hypertrophy) in different animal models.

In contrast to FLT-1, KDR increased significantly 3 weeks after TAC compared with control animals as stated above. In Table 2, it is clearly shown that the FLT-1-to-KDR ratio is decreased 3 weeks after TAC and appears to be directly associated with the onset of cardiomyocyte hypertrophy as described by Zhou et al.[28] According to Zhou and colleagues, by supplementing copper, the FLT-1-to-KDR ratio would increase and the myocardial hypertrophy would regress to being a very simple therapy. But whether VEGF drives the cardiomyocyte in hypertrophy, or its regression, depends on the preferential binding of VEGF to either KDR or FLT-1, and depends also on the PKG-1 acitivity.[28]

By contrast, Bae and colleagues confirmed anti-FLT-1 as a potential therapeutic agent for inhibition of tumor growth and metastasis.[29] In this context, sunitinib, a receptor tyrosine-kinase inhibitor, would be a good example of treatment of advanced renal carcinoma, refractory gastrointestinal stromal tumors and malignant gliomas.[30] By contrast, as these growth factors and receptors play a crucial role in angiogenesis, a key question is whether the administration of proangiogenic agents together with FLT-1 would lead to increasing capillary density.

In this experiment, HIF-1 showed only marginal alteration in a slightly increased gene expression 1 day and 3 weeks after TAC, whereas HIF-2 decreased significantly weekly after week 1 ($p = 0.005$) to week 25 ($p < 0.004$) compared with sham. These results are partly consistent with those of Choi and colleagues, published previously,[7] demonstrating the proangiogenic response in the hypertrophied myocardium as associated with an increased HIF-1 activity but with no detectable HIF-2 expression.[7] A tentative conclusion at this point would be that HIF-1 is slightly increased but nevertheless, not significantly increased. At this point, it is important to explore the difference in gene-expression analysis: while in this study, gene expression has been analyzed on the messenger-RNA level, the previous results were based on analysis of protein levels. On the other hand, there are differences in animal models used before. In the past, Choi and colleagues[7] used infant rabbits; whereas in this study, we used

adult mice. Considering angiogenic factor HIF-1, there was also a comparable pattern in the gene expression of the receptors VEGF and KDR. Though the relationships were not statistically significant, there has been a parallel trend observed. All three proangiogenic factors were increased on day 1, decreasing slightly at week 1, and then increased continuously at week 2 and 3 before a slight decline of HIF-1 and a statistically significant decrease of VEGF and KDR at week 4.

Furthermore, we show that pressure-overload results in a significant upregulation of VEGF and SDF-1 expression after 1 day subsequently decreased after 1 and 2 weeks, and thereafter, only VEGF was increased again significantly at 3 weeks compared with sham.

The SDF-1 regulates specific steps in new vessel formation. It recruits bone-marrow-derived stem/progenitor cells and induces the release of angiogeneic factors, thereby leading to angiogenesis.[31] SDF-1 and its role in ischemic cardiomyopathy are well studied. The increased expression level of SDF-1 in ischemic tissue results in chemotaxis of inflammatory cells toward the site of injury.[32–34] Furthermore, angiogenesis is induced by VEGF release from endothelial cells after myocardial infarction by binding of SDF-1 to its receptor CXCR4.[35] The elevated VEGF level itself results in enhanced endothelial expression of CXCR4. SDF-1 has also been shown to prevent apoptosis of endothelial progenitor cells after myocardial infarction.[36]

However, there is only limited information about the role of SDF-1 in nonischemic cardiomyopathy. It remains unclear whether the SDF-1/CXCR4 signaling pathway is comparable in nonischemic and ischemic cardiomyopathy. Here, we determined the gene-expression levels of SDF-1 after TAC. Our findings suggest that an upregulation of SDF-1 at week 1 post-TAC, compared with sham animals, must be interpreted as a late event in proangiogeneic compensation. At this point, as stated until the end of the 20th century, while myocardial hypertrophy was considered irreversible, many studies have reported that myocardial hypertrophy may possibly regress with multifactorial interventional approaches.[37–39] Subsequently, a central question that needs addressing in this context is, whether an early therapeutic SDF-1 application may contribute to increasing capillary density and may stimulate VEGF production and release, hence lead to myocardial hypertrophy regression. While many recent studies have already looked at the therapeutic effect of SDF-1 application in ischemic myocardium,[40–42] it remains unclear in nonischemic hypertrophied myocardium.

Moreover, oxidative stress plays an important role in ischemic cardiac tissue and thus is worth further focus; analysis of the role of HIF-1 with oxidative stress in cardiac tissue is especially needed. Pialoux and colleagues found that hypoxia induces oxidative stress *via* an overgeneration of reactive oxygen species.[43] Further, Sadaghianloo and colleagues stated that oxidative stress increases in mouse arteriovenous fistula maturation with increased expression of HIF-1.[44] Ultimately, further research and discovery regarding HIF-1 regulation by oxidative stress is warranted for better understanding of disease development and potential therapeutics for pathologies such as cancer, inflammatory diseases, and ischemia–reperfusion injury.

HIF is a key regulator of genes as a response to hypoxia. In myocardial hypertrophy, the decreased capillary density may lead to tissue hypoxia, inducing HIF-dependent signaling. However, this signal pathway may be interrupted so that not enough HIF is produced.

Limitations of the study

Although we only describe the correlation between the proangiogenic factors and the two major VEGFRs, FLT-1 and KDR, we assume in addition to HIF, which plays an important role in angiogenesis, that the decrease of the FLT-1/KDR ratio may lead to myocardial hypertrophy. We use heart weight and LVEF to evaluate heart failure. In fact, using these parameters to evaluate heart failure opens the arena to further investigation.

A more detailed analysis would be needed to fully understand receptor activation in molecular terms. Future research should focus on determining whether the development of new, highly specific inhibitory drugs for therapeutic implications is possible.

Conclusion

Many of these complex gene expressions that interplay have not yet been sufficiently explored.

HIF-1 and VEGF expression were significantly decreased at 1 week compared with 1 day after TAC. Based on these findings, it may be concluded that the participation of HIF-1 is essential, inducing the expression of VEGF, its receptors and SDF-1, inducing angiogenesis in response to myocardial hypertrophy. Our gene-expression data support HIF-1 playing a key role in angiogenesis.

In animals receiving TAC treatment, there was a relative decrease in capillary density in relation to the resulting contractile LV mass. The mechanism appears to depend on the dysregulation of genes involving angiogenesis signaling. Our results suggest that the reconstitution of the capillary density in the hypertrophic heart may improve the myocardial susceptibility to an ischemia–reperfusion injury.

Acknowledgements

The authors would like to thank Jan Kleimann, Meike Lauer, Samira Karavidic and Laura Wilden for their excellent technical assistance.

Funding

This work was funded in part by the Else Kröner-Fr esenius Foundation and the Elisabeth and Rudolf Hirsch Foundation.

Conflict of interest statement

The authors declare that there is no conflict of interest.

ORCID iDs

Anton Sabashnikov https://orcid.org/0000-0002-6289-1035
Julia Merkle https://orcid.org/0000-0003-4490-8937
Kaveh Eghbalzadeh https://orcid.org/0000-0001-6941-7785
Carolyn Weber https://orcid.org/0000-0002-8490-5549

References

1. Maron BJ. Hypertrophic cardiomyopathy: a systematic review. *JAMA* 2002; 287: 1308–1320.
2. Scolletta S, Carlucci F, Biagioli B, *et al.* NT-proBNP changes, oxidative stress, and energy status of hypertrophic myocardium following ischemia/reperfusion injury. *Biomed Pharmacother* 2007; 61: 160–166.
3. Evsikov AV, Graber JH, Brockman JM, *et al.* Cracking the egg: molecular dynamics and evolutionary aspects of the transition from the fully grown oocyte to embryo. *Genes Dev* 2006; 20: 2713–2727.
4. Ozkan A, Kapadia S, Tuzcu M, *et al.* Assessment of left ventricular function in aortic stenosis. *Nat Rev Cardiol* 2011; 8: 494–501.
5. Ingwall JS. Energy metabolism in heart failure and remodelling. *Cardiovasc Res* 2009; 81: 412–419.
6. Pinamonti B, Merlo M, Nangah R, *et al.* The progression of left ventricular systolic and diastolic dysfunctions in hypertrophic cardiomyopathy: clinical and prognostic significance. *J Cardiovasc Med (Hagerstown)* 2010; 11: 669–77.
7. Choi YH, Cowan DB, Nathan M, *et al.* Myocardial hypertrophy overrides the angiogenic response to hypoxia. *PLoS One* 2008; 3: e4042.
8. Friehs I and Del Nido PJ. Increased susceptibility of hypertrophied hearts to ischemic injury. *Ann Thorac Surg* 2003; 75: S678–S684.
9. Bento CF and Pereira P. Regulation of hypoxia-inducible factor 1 and the loss of the cellular response to hypoxia in diabetes. *Diabetologia* 2011; 54: 1946–1956.
10. Yee Koh M, Spivak-Kroizman TR and Powis G. HIF-1 regulation: not so easy come, easy go. *Trends Biochem Sci* 2008; 33: 526–534.
11. Hirota K and Semenza GL. Regulation of angiogenesis by hypoxia-inducible factor 1. *Crit Rev Oncol Hematol* 2006; 59: 15–26.
12. Ceradini DJ and Gurtner GC. Homing to hypoxia: HIF-1 as a mediator of progenitor cell recruitment to injured tissue. *Trends Cardiovasc Med* 2005; 15: 57–63.
13. Ceradini DJ, Kulkarni AR, Callaghan MJ, *et al.* Progenitor cell trafficking is regulated by hypoxic gradients through HIF-1 induction of SDF-1. *Nat Med* 2004; 10: 858–864.
14. Carmeliet P, Dor Y, Herbert JM, *et al.* Role of HIF-1alpha in hypoxia-mediated apoptosis, cell proliferation and tumour angiogenesis. *Nature* 1998; 394: 485–490.
15. Ziello JE, Jovin IS and Huang Y. Hypoxia-inducible factor (HIF)-1 regulatory pathway and its potential for therapeutic intervention in malignancy and ischemia. *Yale J Biol Med* 2007; 80: 51–60.

16. Richard DE, Berra E and Pouyssegur J. Nonhypoxic pathway mediates the induction of hypoxia-inducible factor 1alpha in vascular smooth muscle cells. *J Biol Chem* 2000; 275: 26765–26771.

17. Vincent KA, Shyu KG, Luo Y, *et al*. Angiogenesis is induced in a rabbit model of hindlimb ischemia by naked DNA encoding an HIF-1alpha/VP16 hybrid transcription factor. *Circulation* 2000; 102: 2255–2261.

18. Hu P, Zhang D, Swenson L, *et al*. Minimally invasive aortic banding in mice: effects of altered cardiomyocyte insulin signaling during pressure overload. *Am J Physiol Heart Circ Physiol* 2003; 285: H1261–H1269.

19. Drey F, Choi Y-H, Neef K, *et al.* Noninvasive in vivo tracking of mesenchymal stem cells and evaluation of cell therapeutic effects in a murine model using a clinical 3.0 T MRI. *Cell Transplant* 2012; in press.

20. Vogel M, Staller W and Buhlmeyer K. Left ventricular myocardial mass determined by cross-sectional echocardiography in normal newborns, infants, and children. *Pediatr Cardiol* 1991; 12: 143–149.

21. Kaza E, Ablasser K, Poutias D, *et al*. Up-regulation of soluble vascular endothelial growth factor receptor-1 prevents angiogenesis in hypertrophied myocardium. *Cardiovasc Res* 2011; 89: 410–418.

22. Stuttfeld E and Ballmer-Hofer K. Structure and function of VEGF receptors. *IUBMB Life* 2009; 61: 915–922.

23. Seko Y, Takahashi N, Shibuya M, *et al*. Pulsatile stretch stimulates vascular endothelial growth factor (VEGF) secretion by cultured rat cardiac myocytes. *Biochem Biophys Res Commun* 1999; 254: 462–465.

24. Petrova TV, Makinen T and Alitalo K. Signaling via vascular endothelial growth factor receptors. *Exp Cell Res* 1999; 253: 117–130.

25. Dor Y, Djonov V, Abramovitch R, *et al*. Conditional switching of VEGF provides new insights into adult neovascularization and pro-angiogenic therapy. *EMBO J* 2002; 21: 1939–1947.

26. Shibuya M. Differential roles of vascular endothelial growth factor receptor-1 and receptor-2 in angiogenesis. *J Biochem Mol Biol* 2006; 39: 469–478.

27. Reynolds AR, Reynolds LE, Nagel TE, *et al*. Elevated Flk1 (vascular endothelial growth factor receptor 2) signaling mediates enhanced angiogenesis in beta3-integrin-deficient mice. *Cancer Res* 2004; 64: 8643–8650.

28. Zhou Y, Bourcy K and Kang YJ. Copper-induced regression of cardiomyocyte hypertrophy is associated with enhanced vascular endothelial growth factor receptor-1 signalling pathway. *Cardiovasc Res* 2009; 84: 54–63.

29. Bae DG, Kim TD, Li G, *et al*. Anti-flt1 peptide, a vascular endothelial growth factor receptor 1-specific hexapeptide, inhibits tumor growth and metastasis. *Clin Cancer Res* 2005; 11: 2651–2661.

30. Dimitropoulos K, Giannopoulou E, Argyriou AA, *et al*. The effects of anti-VEGFR and anti-EGFR agents on glioma cell migration through implication of growth factors with integrins. *Anticancer Res* 2010; 30: 4987–4992.

31. Salcedo R and Oppenheim JJ. Role of chemokines in angiogenesis: CXCL12/SDF-1 and CXCR4 interaction, a key regulator of endothelial cell responses. *Microcirculation* 2003; 10: 359–370.

32. McGrath KE, Koniski AD, Maltby KM, *et al*. Embryonic expression and function of the chemokine SDF-1 and its receptor, CXCR4. *Dev Biol* 1999; 213: 442–456.

33. Pillarisetti K and Gupta SK. Cloning and relative expression analysis of rat stromal cell derived factor-1 (SDF-1)1: SDF-1 alpha mRNA is selectively induced in rat model of myocardial infarction. *Inflammation* 2001; 25: 293–300.

34. Yamani MH, Ratliff NB, Cook DJ, *et al*. Peritransplant ischemic injury is associated with up-regulation of stromal cell-derived factor-1. *J Am Coll Cardiol* 2005; 46: 1029–1035.

35. Hu X, Dai S, Wu WJ, *et al*. Stromal cell derived factor-1 alpha confers protection against myocardial ischemia/reperfusion injury: role of the cardiac stromal cell derived factor-1 alpha CXCR4 axis. *Circulation* 2007; 116: 654–663.

36. Takahashi M, Li TS, Suzuki R, *et al*. Cytokines produced by bone marrow cells can contribute to functional improvement of the infarcted heart by protecting cardiomyocytes from ischemic injury. *Am J Physiol Heart Circ Physiol* 2006; 291: H886–H893.

37. Costanzo P, Savarese G, Rosano G, *et al*. Left ventricular hypertrophy reduction and clinical events. A meta-regression analysis of 14 studies in 12,809 hypertensive patients. *Int J Cardiol* 2013; 167: 2757–2764.

38. Goncalves A, Marcos-Alberca P, Almeria C, *et al*. Acute left ventricle diastolic function improvement after transcatheter aortic valve implantation. *Eur J Echocardiogr* 2011; 12: 790–797.

39. Vizzardi E, D'Aloia A, Fiorina C, *et al*. Early regression of left ventricular mass associated with diastolic improvement after transcatheter aortic valve implantation. *J Am Soc Echocardiogr* 2012; 25: 1091–1098.

40. Saxena A, Fish JE, White MD, *et al*. Stromal cell-derived factor-1alpha is cardioprotective after myocardial infarction. *Circulation* 2008; 117: 2224–2231.

41. Kanki S, Segers VF, Wu W, *et al*. Stromal cell-derived factor-1 retention and cardioprotection for ischemic myocardium. *Circ Heart Fail* 2011; 4: 509–518.

42. Sundararaman S, Miller TJ, Pastore JM, *et al*. Plasmid-based transient human stromal cell-derived factor-1 gene transfer improves cardiac function in chronic heart failure. *Gene Ther* 2011; 18: 867–873.

43. Pialoux V, Brugniaux JV, Fellmann N, *et al*. Oxidative stress and HIF-1 alpha modulate hypoxic ventilatory responses after hypoxic training on athletes. *Respir Physiol Neurobiol* 2009; 167: 217–220.

44. Sadaghianloo N, Yamamoto K, Bai H, *et al*. Increased oxidative stress and hypoxia inducible factor-1 expression during arteriovenous fistula maturation. *Ann Vasc Surg* 2017; 41: 225–234.